

## Communications to the Editor

### Acid Distribution in Phosphonic Acid-Doped Polyaniline by Solid-State NMR

Tanya L. Young, Jennifer L. Cross, and  
Matthew P. Espe\*

Department of Chemistry, Knight Chemical Laboratory,  
University of Akron, Akron, Ohio 44325

Received August 8, 2002

**Introduction.** Polyaniline (PANI), an organic conducting polymer, is converted from its insulating (undoped) form to its conducting (doped) by simple protonation, in contrast to most other conducting polymers that are doped by oxidation or reduction. The polymer has realized or proposed applications in the areas of RF shielding, corrosion protection, batteries, actuators, and LED's as well as a number of other fields. The substantial interest in PANI results from its ease of synthesis and processing and its chemical stability in both the insulating and conducting forms. The conductivity of PANI can be tuned over  $\sim 8$  orders of magnitude by varying the acid used for doping and the solvent from which the material is processed. The higher conductivities are realized when organic acids are used as the dopant.<sup>1</sup> The highest conductivity ( $\sigma \sim 400$  S/cm) is observed when camphorsulfonic acid (HCSA) is the dopant and *m*-cresol is the solvent,<sup>2</sup> and the conductivity of this material increases to  $\sim 1000$  S/cm upon stretching the PANI film.<sup>3</sup> While the conductivity of PANI is below those of metals such as Cu ( $\sigma = 10^5$  S/cm), Epstein and co-workers have proposed that the intrinsic conductivity is  $\sim 10^7$  S/cm.<sup>4</sup> The limitation to reaching this maximum value is the inherent disorder present in the glassy polymer.

The conductivity of HCSA-doped PANI films cast from *m*-cresol is also a function of doping level. The conductivity of the undoped material is  $\sim 10^{-10}$  S/cm, and this

value increases dramatically to 0.7 S/cm at *only* a 20% doping level, to 92 S/cm at 60% doping, and finally to 179 S/cm in the fully doped material, showing that substantial conductivity is observed even when the system is well below fully doped levels.<sup>5</sup> The variation of conductivity with doping level is likely related to the distribution of protonation sites within the polymer. The distribution of the protonation sites in HCl doped PANI has been observed to be heterogeneous, with the doping preferentially occurring in the amorphous phase followed by doping into the crystalline domains.<sup>6</sup> Similarly, a solid-state NMR (SSNMR) characterization of HF doped PANI showed preferential doping of the amorphous regions over more ordered regions, at lower doping levels.<sup>7</sup> A similar characterization of the arrangement of doping sites in an organic acid doped PANI has not been undertaken.

This report describes our studies of the distribution of an organic acid in PANI at various doping levels. The acid chosen in this study is *tert*-butylphosphonic acid (TBPA) as the acid moiety itself can be readily monitored by NMR. The acid distribution is investigated by measuring  $^{31}\text{P}$ – $^{31}\text{P}$  dipolar coupling by using the SSNMR dipolar recoupling technique of DRAMA.<sup>8</sup> The  $^{31}\text{P}$ – $^{31}\text{P}$  distances, determined from the dipolar couplings, provide insights into the distribution of the acid molecules in TBPA doped PANI at various doping levels.

**Experimental Section.** Cross-polarization, magic-angle spinning  $^{13}\text{C}$  and  $^{31}\text{P}$  spectra were obtained on a Chemagnetics/Tecmag system operating at 4.7 T.<sup>9</sup> The  $H_1$  field was 50 kHz for the observe nucleus, with proton decoupling at 85 kHz. The DRAMA sequence contained eight equally spaced  $\pi$  pulses per rotor period to remove frequency offsets and two  $\pi/2$  pulses at  $1/4$  and  $3/4$  of the rotor period for dipolar recoupling.<sup>10</sup> The pulses were phase cycled using the XY-8 scheme.<sup>11</sup> Polyaniline (Neste Oy) was mixed with TBPA (Aldrich) and then dissolved in *N*-methylpyrrolidinone (NMP, Aldrich) to make a 1% w/w solution. The solution was filtered with a 0.45  $\mu\text{m}$  filter (Whatman:PTFE) and placed in a vacuum oven at 75 °C until dry,  $\sim 5$  h. The diphen-

\* Corresponding author: phone 330-972-6060; Fax 330-972-7370; e-mail Espe@uakron.edu.

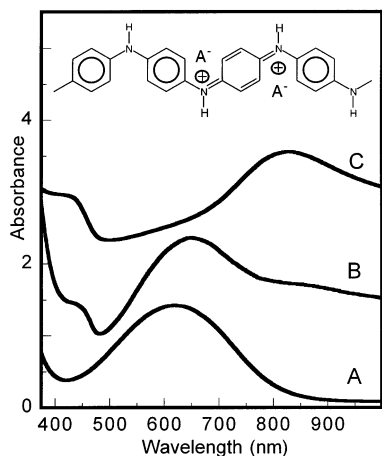


**Figure 1.** UV/vis spectra from thin films of TBPA:PANI cast from NMP. The TBPA:PANI mole ratio in solution is (A) 0, (B) 0.5, and (C) 2.0. The acid to PANI mole ratios are based on the four-ring repeat unit of PANI. The thin films are formed by placing a small volume of the solution on a glass slide and drying at 75 °C under vacuum for ~5 h. Insert: repeat unit of fully doped PANI (2:1 acid to PANI mole ratio);  $A^-$  is the acid anion.

ylphosphine-substituted polystyrene (Strem) was used as received.

**Results and Discussion.** TBPA:PANI films were cast from NMP solutions that contained no TBPA (undoped), TBPA in a 0.5:1 molar ratio with PANI (25% doped), or a TBPA:PANI ratio of 2 (fully doped). XRD characterization of the films showed that they are completely amorphous. Similar to the HCSA-doped PANI, the conductivity of the 25% doped film was ~10% that of the fully doped film with a room temperature conductivity of  $10^{-5}$  S/cm, as measured by using the four-probe method. The UV/vis spectrum from the fully doped PANI film (Figure 1C), absent the peak at 640 nm from the undoped polymer (Figure 1A) and with a  $\lambda_{\max}$  at ~850 nm, is consistent with the polymer being fully doped and having a compact-coil conformation.<sup>12</sup> The UV/vis spectrum from the 25% doped film has peaks at both 640 and 850 nm (Figure 1B), indicating that at this doping level PANI consists of both doped and undoped domains. Figure 2 shows the  $^{13}\text{C}$  SSNMR spectra from PANI films cast from NMP solutions that contain no TBPA or TBPA present in 0.5:1 and 2:1 molar ratios. The spectrum from the fully doped material (Figure 2C) consists of a broad, almost featureless peak, as has been reported previously for fully doped PANI.<sup>7,13</sup> The line broadening is a result of the charge distribution heterogeneity along the polymer chain, resulting from structural disorder of the polymer chains in the solid state.<sup>13</sup> When partially doped, the  $^{13}\text{C}$  spectrum (Figure 2B) has features similar to that observed for the PANI film, however with broader lines. Underlying the sharper peaks is a broad peak, observable in the regions near ~100 and 150 ppm, similar to that seen for the fully doped polymer. The  $^{13}\text{C}$  NMR and UV/vis data show that PANI is fully doped at a TBPA:PANI ratio of 2 and that the polymer does not become fully doped until the 2:1 mole ratio is reached. These results show that TBPA does not act as a diprotic acid to any significant extent and that all the TBPA present is involved in protonating the polymer.

In the DRAMA experiment two spectra are obtained: one with the dipolar coupling between phosphorus nuclei averaged to zero by magic-angle spinning, with

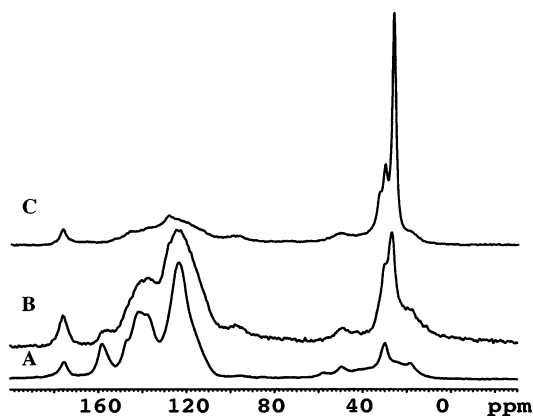


**Figure 2.**  $^{13}\text{C}$  CP/MAS spectra of (A) PANI cast from NMP, (B) TBPA:PANI (0.5:1) cast from NMP, and (C) TBPA:PANI (2:1) cast from NMP. Peaks in the aliphatic region of the spectra and at 175 ppm arise from retained NMP. These peaks are most readily observed in the undoped PANI film. In the doped films the peaks at 30–40 ppm arise from TBPA. Sample spinning speed is 5 kHz.

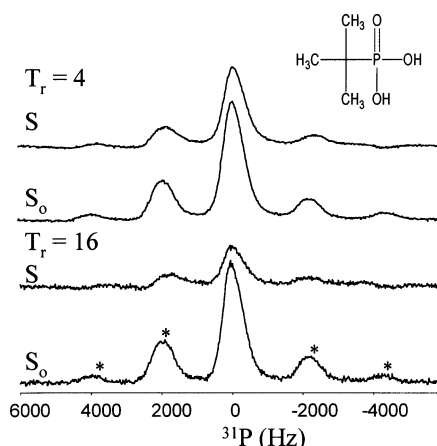


**Figure 3.**  $S$  and  $S_0$   $^{31}\text{P}$  DRAMA spectra from TBPA:PANI (2:1) with 4 rotor period of dipolar recoupling (top) and 16 rotor periods of dipolar recoupling (bottom). Inset: structure of TBPA. Sample spinning speed was 2083 Hz for all DRAMA experiments. \* = spinning sidebands.

integrated intensity  $S_0$ , and the second with the dipolar coupling reintroduced by the application of two  $\pi/2$  pulses per rotor period, with intensity  $S$ . The change in  $S/S_0$  with the number of rotor periods of applying the  $\pi/2$  pulses is a function of the strength of the  $^{31}\text{P}$ – $^{31}\text{P}$  dipolar coupling. The  $S$  and  $S_0$   $^{31}\text{P}$  spectra from fully doped PANI with 4 and 16 rotor period DRAMA are shown in Figure 3. While amplitude and phase distortions can occur in the data in the case of large chemical shift anisotropies,<sup>8</sup> with the smaller chemical shift tensor of the  $^{31}\text{P}$  in TBPA, these distortions are not expected,<sup>10,14</sup> and the spectra of Figure 3 show no phase distortions.

The values of  $S/S_0$  for 25% and 100% doped PANI are shown in Figure 4. The similarity of the DRAMA results for the two PANI films implies that the arrangement of the acid molecules is very similar in the two materials. Thus, even when doped to 25% of the fully doped level, the interacid distance is the same as observed for the fully doped material. A random distribution of the acid molecules throughout a partially doped PANI sample would yield both long and short  $^{31}\text{P}$ – $^{31}\text{P}$  distances. This is the case for  $p$ -diphenylphos-

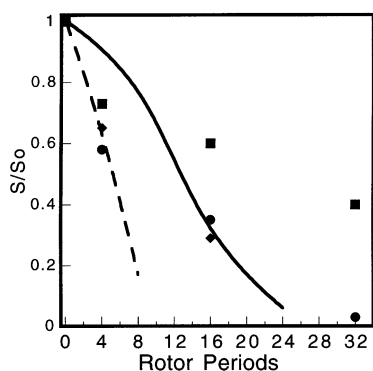


**Figure 4.** Value of  $S/S_0$  at various number of rotor periods for TBPA:PANI (0.5:1) (◆), TBPA:PANI (2:1) (●), and DPP-PS (■). The values of  $S$  and  $S_0$  were determined from integrating over the isotropic peak and the spinning sidebands. Simulation results for dipolar couplings of 275 Hz ( $r = 4.1$  Å) (---) and 110 Hz ( $r = 5.6$  Å) (—) are also plotted on the graph. The simulations included the use of finite pulse widths and the full chemical shift anisotropy of  $^{31}\text{P}$ .

phine polystyrene (DPP-PS), where  $\sim 10\%$  of the repeat units (randomly distributed) of polystyrene have been substituted at the para position with diphenylphosphine groups. The distribution of  $^{31}\text{P}$ – $^{31}\text{P}$  distances in DPP-PS is revealed in the DRAMA data (Figure 4). Simulation of the DRAMA data by using the SIMPSON<sup>15</sup> package indicates a  $^{31}\text{P}$  internuclear distance of  $\sim 4$  Å from the 4 rotor period experiment, with the distance extending to  $\sim 10$  Å for the 32 rotor period results. In contrast, simulation of the TBPA:PANI data is possible by using an internuclear distance of  $5 \pm 1$  Å to account for all the data from both the partially and fully doped PANI samples (Figure 4). The DRAMA data indicate that at low doping levels the TBPA is not randomly distributed throughout the polymer but rather is located in domains that become fully doped, accounting for the similarity of the DRAMA data from the two PANI samples. This then leaves other portions (domains) of the polymer in the completely undoped form, a model also consistent with the UV/vis and  $^{13}\text{C}$  data.

The interacid distance of TBPA of  $\sim 5$  Å is slightly shorter than those determined for inorganic acid-doped PANI. X-ray diffraction studies of HCl-doped PANI showed that the distance between  $\text{Cl}^-$  is 6.3 Å in the crystalline regions of the film.<sup>16</sup> The NMR determined distance between  $\text{F}^-$  in HF doped PANI is similar at  $\sim 6.5$  Å.<sup>7</sup> However, direct comparison with the TBPA results is complicated by the fact that the DRAMA

simulations assumed the presence of only isolated  $^{31}\text{P}$  spin pairs. In the TBPA-doped PANI each  $^{31}\text{P}$  may have several nearest-neighbor phosphorus nuclei, and the simulation results becomes model dependent, as both distance and relative orientation of the nuclei involved must be considered. Experiments are underway to obtain additional distance constraints to allow for the construction of realistic models to be used as the input parameters for the simulations. The goal of this work being the construction of an accurate description of the structure of the TBPA:PANI system.

**Conclusion.** The heterogeneous distribution of TBPA in PANI accounts for the relatively high conductivity previously observed at low (20%) doping levels.<sup>5</sup> The domains that are fully doped will then have conductivities similar to those of the fully doped material, with the undoped regions remaining as insulators. Connectivity of these conducting domains within the polymer sample then provides the pathway for the electrical conductivity.

## References and Notes

- (1) Cao, Y.; Qiu, J.; Smith, P. *Synth. Met.* **1995**, *69*, 187.
- (2) Cao, Y.; Smith, P.; Heeger, A. J. *Synth. Met.* **1992**, *48*, 91.
- (3) Abell, L.; Adams, P. N.; Monkman, A. P. *Polymer* **1996**, *37*, 5927.
- (4) Kohlman, R. S.; Zibold, A.; Tanner, D. B.; Ihas, G. G.; Ishiguro, T.; Min, Y. G.; MacDiarmid, A. G.; Epstein, A. J. *Phys. Rev. Lett.* **1997**, *78*, 3915.
- (5) Avlyanov, J. K.; Yonggang, M.; MacDiarmid, A. G.; Epstein, A. J. *Synth. Met.* **1995**, *72*, 65.
- (6) Jozefowicz, M. E.; Laversanne, R.; Javadi, H. H. S.; Epstein, A. J.; Pouget, J. P.; Tang, X.; MacDiarmid, A. G. *Phys. Rev. B* **1989**, *39*, 12958.
- (7) Espe, M. P.; Mattes, B. R.; Schaefer, J. *Macromolecules* **1997**, *30*, 6307.
- (8) Tycko, R.; Dabbagh, G. *Chem. Phys. Lett.* **1990**, *173*, 461.
- (9) Young, T. L.; Yang, D.; Mattes, B. R.; Espe, M. P. *Macromolecules* **2002**, *35*, 5565.
- (10) Klug, C. A.; Zhu, W.; Merritt, M. E.; Schaefer, J. *J. Magn. Reson., Ser. A* **1994**, *109*, 134.
- (11) Gullion, T.; Baker, D.; Conradi, M. S. *J. Magn. Reson.* **1990**, *89*, 479.
- (12) Xia, Y.; Wiesinger, J. M.; MacDiarmid, A. G.; Epstein, A. J. *Chem. Mater.* **1995**, *7*, 443.
- (13) Kaplan, S.; Conwell, E. M.; Richter, A. F.; MacDiarmid, A. G. *J. Am. Chem. Soc.* **1988**, *110*, 7647.
- (14) Tycko, R.; Smith, S. O. *J. Chem. Phys.* **1993**, *98*, 932.
- (15) Bak, M.; Rasmussen, J. T.; Nielsen, N. C. *J. Magn. Reson., Ser. A* **2000**, *147*, 296.
- (16) Pouget, J. P.; Jozefowicz, M. E.; Epstein, A. J.; Tang, X.; MacDiarmid, A. G. *Macromolecules* **1991**, *24*, 779.

MA021282L